By Frank V. Bright
Department of Chemistry
Natural Sciences and Mathematics Complex
State University of New York at Buffalo
Buffalo, New York 14260-3000

Modern Molecular Fluorescence Spectroscopy

INTRODUCTION

On absorption of electromagnetic radiation, the fate and pathway of a molecule back to the ground state are dictated by its inherent structure and the physiochemical properties of its local environment. In some situations, one or more of the pathways back to the ground state involve emission of electromagnetic radiation. When this emission is from a singlet state the process is termed fluorescence.

Fluorescence is unique among spectroscopic techniques because it is inherently multidimensional.[1-7] That is, the emission process contains a wealth of orthogonal information that is related to the fluorophore and its surroundings. Specifically, one can conveniently divide fluorescence into its static and dynamic forms. These categories can be further divided into subcategories with particular features:

Static

Intensity

- Concentration of species.
- Quenching of species (molecular accessibility, conformational changes, kinetics of change).

Spectral

- Information on the local environment surrounding the fluorophore (e.g., polarity, pH).
- Number of emitting components.
- Average distance between sites by determining energy transfer.

Polarization/Anisotropy

- Average size of a rotationally mobile species.
- Mobility or motional restriction.
- Protein–ligand binding.

Dynamic

Excited-State Intensity Decay

- Resolve static emission into contributions from the individual emissive centers.
- Study ultrafast kinetic processes (e.g., solvation).
- Unravel excited-state decay kinetics.
- Elucidate origin of quenching processes.
- Study exchange processes and heterogeneity (e.g., continuous lifetime distributions).

Excited-State Decay of Anisotropy

- Detailed reorientational dynamics of nonspherical rotors.
- Overall shape of the rotating body.
- Discrimination between local and global motions in a complex system.
- Determine how surfaces affect the mobility of model solutes.

The goal of this tutorial is to present the concepts of modern molecular fluorescence spectroscopy and provide a foundation for extricating key information from static and dynamic fluorescence data. Selected examples from the literature are mentioned briefly within each subsection; however, the discussion is not necessarily exhaustive. Additional details and examples can be found in several excellent books,[1-3] in reviews,[4-7] and in many of the papers that appear in this issue of *Applied Spectroscopy*.

Static Spectroscopy. Figure 1 presents a simplified energy-level diagram for a hypothetical aromatic molecule. On absorption (ABS′ or ABS″)

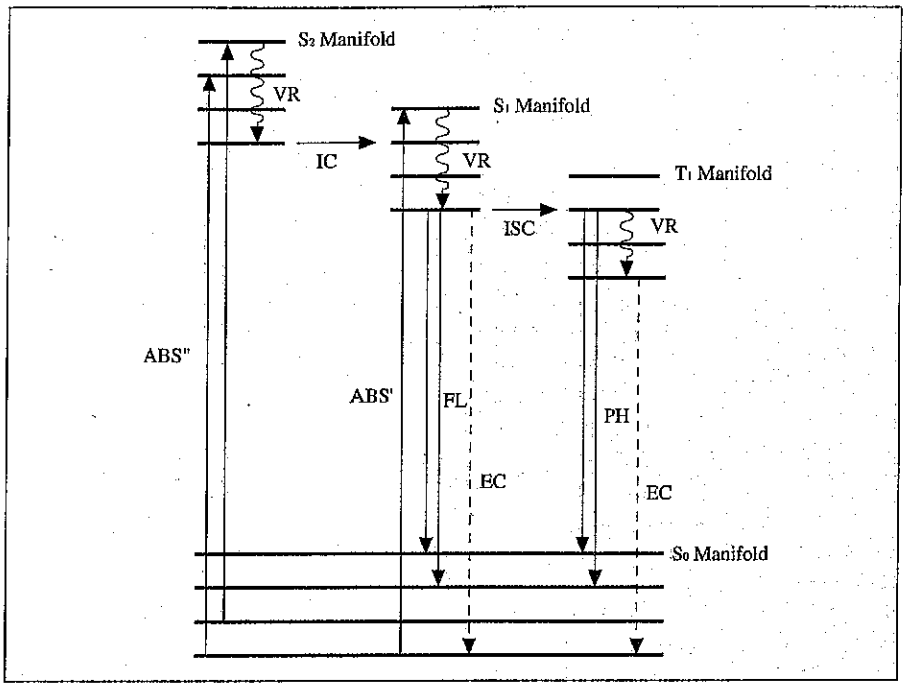

FIG. 1. Simplified energy-level diagram for an aromatic chromophore. See text for definition of terms.

from the ground singlet manifold (S_0), a molecule is promoted, within a few femtoseconds, to an excited singlet state (e.g., S_1 or S_2). (Several vibrational levels are shown within each single manifold, and rotational levels are omitted for clarity.) Relaxation back to the ground state can involve vibrational relaxation (VR), internal conversion (IC), external conversion (EC), intersystem crossing (ISC) from the singlet to the triplet (T_1) manifold, emission from T_1 to S_0 (phosphorescence, PH), and/or singlet-to-singlet emission–fluorescence (FL).

The fluorescence excitation and emission spectra (intensity vs. wavelength or energy) provide one with a relative measure of the energy associated with individual transitions or groups of transitions, the probability of efficiency of individual transitions with respect to one another, information (with certain calibration schemes) on the absolute efficiency of a given process, and information on the *average* physicochemical properties of the environment surrounding the fluorescent probe (i.e., the cybotactic region). For dilute solutions, the observed fluorescence signal Fl is given by:

$$Fl = kP_0C \tag{1}$$

where k is an instrument factor, P_0 is the radiant power of the source used to excite the sample, and C is the analytical concentration of the fluorophore.

Static fluorescence has been used to resolve complex mixtures into the contributions from individual components,[8] to quantify nonfluorescent analytes,[9] to determine the physiocochemical properties of the local environment surrounding a fluorescent reporter group,[10] to probe biointerfaces,[11] and to detect single molecules.[12,13]

Static Fluorescence Polarization or Anisotropy. In a fluorescence polarization (anisotropy) experiment, one excites the sample with polarized electromagnetic radiation and monitors the parallel ($Fl_\parallel$) and perpendicular ($Fl_\perp$) components of the fluorescence.[1,2] The fluorescence anisotropy (r) is then written as:

$$r = \frac{(Fl_\parallel - Fl_\perp)}{(Fl_\parallel - 2Fl_\perp)}. \tag{2}$$

Photoselection results in the fluorescence being partially polarized to an extent that depends (in the simplest scenario) on the angular orientation between the absorbance and emission transition moments, the excited-state lifetime, and the rate of rotational diffusion.

If rotational diffusion is the main cause of anisotropy loss, the observed anisotropy is given by the Perrin expression:

$$r = \frac{r_0}{1 + \frac{\tau}{\phi}} \tag{3}$$

where r_0 is the limiting anisotropy obtained when the fluorophore is dissolved in a vitrified solvent, τ is the excited-state fluorescence lifetime (*vide infra*), and ϕ is the rotational correlation time. For a spherical rotor, the rotational correlation time is related to the solvent viscosity (η) and molar volume (V) of the reorienting entity:

$$\phi = \frac{\eta V}{RT} \tag{4}$$

where R and T represent the gas constant and Kelvin temperature, respectively.

Fluorescence anisotropy measurements have been used to probe membrane structure and fluidity,[14] to determine the mobility of solutes at interfaces,[15] to quantify the mean distance between donors and acceptors,[16] to develop homogeneous immunoassays,[17] to follow the aging of inorganic glass composites,[18] and to investigate molecular-level interactions in supercritical fluids.[19]

Intensity Decay Kinetics. *Time Domain.* If the excitation source is rapidly turned off, the intensity from the fluorescent species decays as the excited state becomes depleted of excited fluorophores.[1–5,20] The time course of this process is often described by an exponential decay law of the form:

$$Fl(t) = Fl_0 e^{-t/\tau} \tag{5}$$

where Fl_0 is the fluorescence intensity at the time excitation is terminated, and τ is the excited-state fluorescence lifetime. In many cases the intensity decay is not accurately described by a single exponential decay law. In these situations the observed decay is generally given by a sum of exponentials:

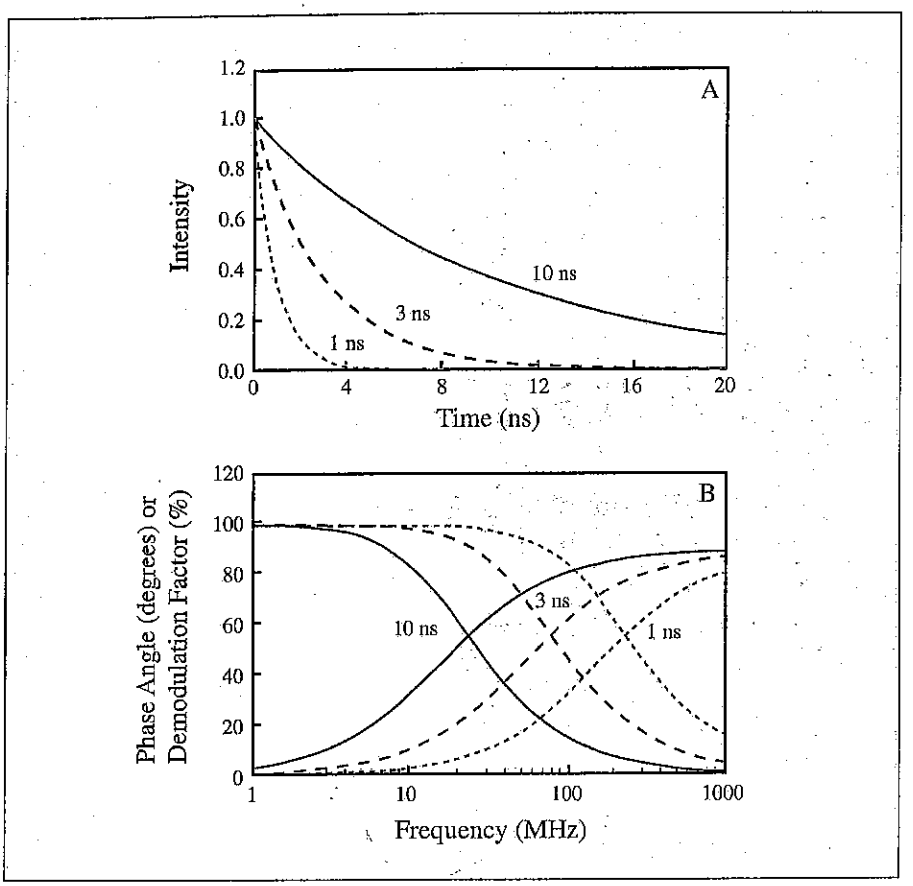

FIG. 2. Simulated time-domain (panel A) and frequency-domain (panel B) traces for 1-, 3-, and 10-ns fluorescence lifetime. The data in panel A have been deconvolved; there is no instrument response function. In panel B, the phase angle increases and the demodulation factor decreases with increasing frequency.

$$Fl(t) = \sum_{i=1}^{n} \alpha_i e^{-t/\tau_i} \qquad (6)$$

where α_i is the pre-exponential factor denoting the fractional contribution to the total time-resolved decay of the component with lifetime τ_i. More recently, it has become popular to use kinetic models represented by distributions of decay times [i.e., $\alpha(\tau)$] in an effort to more accurately describe the observed decay profiles.[21,22]

Simple time-domain decay profiles (Fig. 2A) arise only if the sample is excited with a δ-function (infinitely short) pulse of light. Most real situations involve an excitation pulse and/or an instrument response function that are on the same order of time as the fluorescence process. Under these circumstances, the sought-after fluorescence response [$Fl(t)$] is convolved with the instrument response function [$I(t)$] so that one obtains an observed [$O(t)$] decay profile of the form:

$$O(t) = \int_0^t I(t')Fl(t - t')\,dt'. \qquad (7)$$

The goal is then to extract $Fl(t)$ and, in turn, the kinetic parameters from the experimental measurables [$O(t)$ and $I(t)$].

Numerous methods exist to obtain $Fl(t)$ from $O(t)$ and $I(t)$.[23] Most, however, use least-squares methods in concert with an iterative reconvolution scheme. In this approach, one picks a test model (Eq. 6). The convolution integral (Eq. 7) is then calculated on the basis of an initial set of α_i and τ_i values and the measured instrument response function. The calculated response [$C(t)$] is compared with the observed data [$O(t)$] and the α_i and τ_i terms adjusted until a best fit is obtained. The quality of the fit is judged by chi-squared (χ^2) test:

$$\chi^2 = \sum_{j=1}^{np} W_j[O(t) - C(t)]^2 \qquad (8)$$

where np is the number of data points in the decay file, and W_j is a weighting factor. If the data are obtained with the use of time-correlated single photon counting methods, W_j follows Poisson statistics.[20,23]

Frequency Domain. In the frequency domain, the sample is excited with sinusoidally modulated light, and the experimentally measured parameters are the frequency-dependent phase shift [$\Psi(\omega)$] and modulation [$M(\omega)$].[24–26] These values are compared by nonlinear regression to the values predicted from an assumed decay law, and the parameters of the model adjusted to yield minimal deviations between the data and the prediction. For any time-domain decay law (Eq. 6), the frequency-domain data are related by the sine and cosine Fourier transforms:

$$S(\omega) = \frac{\int Fl(t)\sin\omega t\,dt}{\int Fl(t)\,dt} \qquad (9)$$

$$C(\omega) = \frac{\int Fl(t)\cos\omega t\,dt}{\int Fl(t)\,dt} \qquad (10)$$

where ω is the angular modulation frequency ($\omega = 2\pi f$, f = linear modulation frequency). These are related to the experimentally measured parameters:

$$\Psi(\omega) = \arctan[S(\omega)/C(\omega)] \qquad (11)$$

$$M(\omega) = [S(\omega)^2 + C(\omega)^2]^{1/2}. \qquad (12)$$

The decay terms (α_i and τ_i) are recovered by minimization of the χ^2 function:

$$\chi^2 = \frac{1}{D}\sum\left(\frac{\Psi(\omega) - \Psi_c(\omega)}{\delta\Psi}\right)^2 + \frac{1}{D}\sum\left(\frac{M(\omega) - M_c(\omega)}{\delta M}\right)^2. \qquad (13)$$

In this expression D is the number of degrees of freedom, and $\delta\Psi$ and δM are the uncertainties in the measured phase and modulation, respectively. The subscript c denotes the frequency-dependent phase and modulation calculated on the basis of α_i and τ_i. Figure 2B illustrates the sort of frequency-domain traces one would recover for a fluorophore exhibiting a 1-, 3-, and 10-ns excited-state lifetime. These are compared with the corresponding time-resolved decay profiles in Fig. 2A.

Time-and frequency-domain fluorescence have been used to determine the origin of complex emission processes associated with amino acid residues in proteins,[27] to follow the reorganization of dipoles surrounding fluorescent reporter groups,[28] to study organized media (micelles, cyelodextrins, etc.),[29] to follow fast chemical reactions (e.g., the rate of deprotonation),[30,31] to study quenching mechanisms,[32,33] to study solvent effects on polymer tail-to-tail dynamics,[34] to determine the thermodynamics associated with model biosensor interfaces and resolve the total emission from complex immunosurfaces,[35–37] and to probe "reactions" in supercritical fluids.[38,39]

Anisotropy Decay Kinetics. *Time Domain.* In the time domain the sample is excited with a brief pulse of polarized light, and the time dependence of the parallel $[Fl_{\parallel}(t)]$ and perpendicular $[Fl_{\perp}(t)]$ components of the fluorescence yields the time-resolved decay of anisotropy $r(t)$:

$$r(t)=\frac{(Fl_{\parallel}(t)-Fl_{\perp}(t))}{(Fl_{\parallel}(t)+2Fl_{\perp}(t))}. \qquad (14)$$

For a simple isotropic rotor, $r(t)$ decays with a single rotational correlation time, ϕ:[1,2,20,23]

$$r(t) = r_0\exp(-t/\phi). \qquad (15)$$

For more complicated systems, $r(t)$ takes the form of a sum of exponentials:

$$r(t) = r_0 \Sigma \beta_i \exp(-t/\phi_i) \qquad (16)$$

where β_i and ϕ_i are the fractional contribution of the total depolarization and the rotational correlation times attributed to reorientational motion, i, respectively.

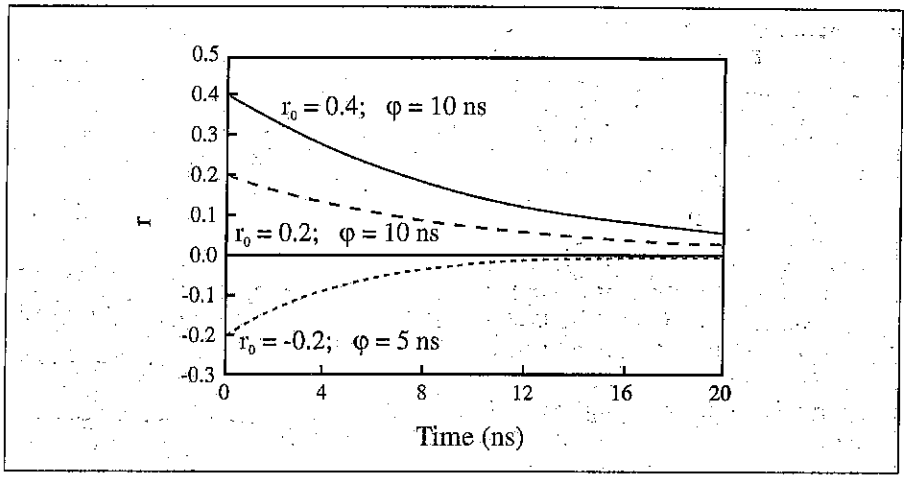

FIG. 3. Simulated time-resolved anisotropy decay profiles for several representative values of limiting anisotropy (r_0) and rotational correlation time (ϕ). In these particular simulations, the time-dependent decay of anisotropy [r(t)] is given by $r_0e^{-t/\phi}$.

The kinetic terms are recovered with the use of any one of several analysis protocols.[23] A series of simulated time-domain anisotropy decay profiles are shown in Fig. 3. These particular examples show the time evolution of the anisotropy decays with rotational correlation times given by ϕ. Immediately following photoexcitation, the fluorophore has yet to reorient, and the observed anisotropy should be equal to r_0 (the limiting anisotropy). As time passes, the molecules reorient and the anisotropy decays toward zero. (If the rotational motion is hindered or otherwise restricted, one would see that the anisotropy does not decay to zero.) In these particular examples, limiting anisotropies of 0.4, 0.2, and −0.2 might result from photoexcitation at different wavelengths (r_0 depends on the relative orientation of the absorption and emission transition moments) for the same fluorophore or from inherent differences in the molecular transition moment structure if we are comparing different fluorophores. For example, the two decay traces with the 10-ns rotational correlation time and different r_0 values could result from exciting the *same* fluorophore/system, undergoing isotropic rotational reorientation, at two different excitation wavelengths so that r_0 is 0.4 or 0.2. In contrast, the trace described by the 5-ns rotational correlation time, if it reflects a single fluorophore undergoing isotropic rotational reorientation, must be from a *different* fluorophore/system from the one for 10-ns species.

Frequency Domain. Rotational reorientation kinetics are also determined from frequency-dependent measurements of the differential polarized phase angle Δ $(= \theta_{\perp} - \theta_{\parallel})$ and the polarized modulation ratio Λ $(=m_{\parallel}/m_{\perp})$.[1,2,24–26]

If the time-dependent decay is given by Eq. 6, the decay of the parallel and perpendicular components of the polarized fluorescence is written:

$$Fl_{\parallel}(t) = \tfrac{1}{3}[Fl(t)(1 + 2r(t)] \qquad (17)$$

and

$$Fl_{\perp}(t) = \tfrac{1}{3}[Fl(t)(1 - r(t))] \qquad (18)$$

where $r(t)$ is the fluorescence anisotropy decay. Regardless of the form of the anisotropy decay, Δ and Λ are given by:

$$\Delta = \arctan\left[\frac{D_{\parallel}N_{\perp} - D_{\perp}N_{\parallel}}{N_{\parallel}N_{\perp} + D_{\perp}D_{\parallel}}\right] \qquad (19)$$

$$\Lambda = \left[\frac{N_{\parallel}^2 + D_{\parallel}^2}{N_{\perp}^2 + D_{\perp}^2}\right]^{1/2} \qquad (20)$$

where N_i and D_i represent the polarized components of the sine and cosine Fourier transforms, respectively. The parameters of interest, β_i and ϕ_i, are subsequently recovered by fitting the frequency-dependent Δ and Λ data

using nonlinear regression methods (*vide supra*). Figure 4 illustrates the frequency-domain traces corresponding to the time-resolved decay profiles shown in Fig. 3. Panels A and B depict the frequency-dependent differential polarized phase angle (Δ) and polarized modulation ratios (Λ), respectively. These types of data would typically be acquired by exciting the sample with sinusoidally modulated light at a *series* of modulation frequencies and measuring the differential phase angle and polarized modulation ratio at *each* frequency.

Time-resolved anisotropies have been used to study the fundamental effects of solvent frictional forces on solute dynamics,[40] to recover the dynamics associated with complex solutes,[41] to probe segmental mobility in proteins,[42] to determine the function of model biorecognition elements/reporter groups over a wide range of conditions (native, denatured, surface adsorbed),[43,44] to study the reorientational mobility of adsorbates at model chromatographic interfaces,[45] and to follow the internal dynamics within protein systems.[46,47]

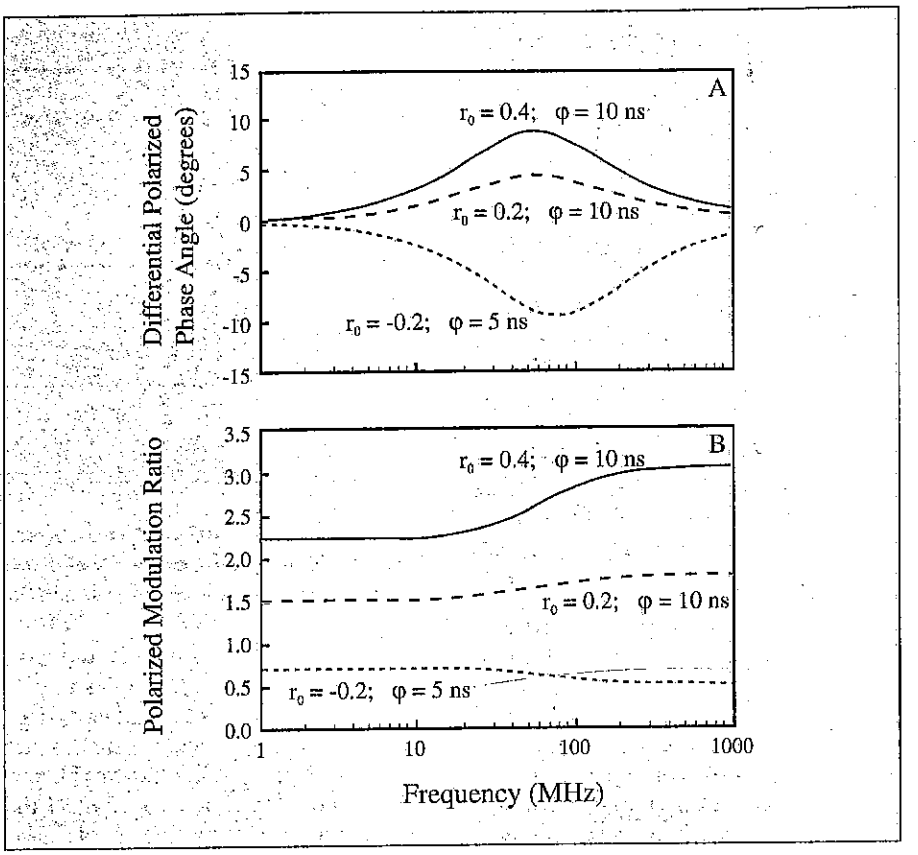

FIG. 4. Simulated differential phase (panel A) and polarized modulation ratio (panel B) traces for the same anisotropy decay profiles illustrated in Fig. 3.

FUTURE

The future of fluorescence spectrometry is indeed promising. Single molecule detection is now a reality, and time-resolved measurements on single molecules have been demonstrated. Femtosecond laser systems and fast electronics, electro-optics, and/or frequency upconversion techniques allow one to directly study femtosecond processes (e.g., solvent relaxation). Thus, it would seem that detection limits and time resolution are nearing their practical limits. The main challenge now is to bring down the cost of this technology and to make the instrumentation more reliable. The solid-state (mode-locked Ti:sapphire) and diode-pumped laser systems will undoubtedly help meet this challenge.

Acquisition times for many fluorescence experiments can become almost prohibitive, and multiplex techniques that allow one to simultaneously acquire spectral, temporal, and polarization information will continue to evolve. Today, it is already possible to acquire reasonable time-and frequency-domain decay traces on the fly in a time frame substantially less than 1 s.

Liquid/liquid, liquid/solid, and solid/solid interfaces are of critical importance to the separation sciences, bioadhesion, protein adsorption, and biosensors. However, only recently has the power of time-resolved fluorescence been directed toward these systems. This trend will certainly continue.

Fluorescence microscopy has already been used to image interfaces and to study desorption and lateral diffusion mechanisms. More recently, fluorescence microscopy has been used in concert with picosecond time resolution. This work will certainly continue, and it should not be too long until one can image intact cells that are labeled with specific fluorescent dyes and/or chelators (e.g., fura-2), and resolve the total emission into contributions from specific sites and or residues within the cell.

It is well known that fluorescence exhibits superb detection limits, and the literature is now ripe with examples of "single molecule detection". As researchers begin to apply this detection technology to real, high-speed problems in, for example, genome sequencing and capillary separations, there will be a push to achieve single molecule detection while maintaining the residence time of the samples within the probe beam volume to an absolute minimum. In this way, one may eventually hope to have single molecule detection in near real time.

Fluorescence is ideally suited for many remote sensing schemes because it is multidimensional and possesses excellent detection limits. Unfortunately, except for a few examples, fluorescence is not used for remote sensing because of the complexity of light sources (e.g., lasers, power supplies, cooling water) and detectors (bulky, power supplies, support electronics). Again, advances in laser technology

and simple, alternative light sources coupled to small, high-gain photodiodes or array detectors should improve this situation soon.

Fluorescence has been known for well over 300 years and has proven to be a viable tool in biology, biochemistry, chemistry, and physics. It will continue to be used in these fields, and, as the cost of the excitation and detection units drop, we should see what are today only research laboratory setups become used more routinely.

ACKNOWLEDGMENTS

The work reported from the author's laboratories was supported by the National Science Foundation (CHE-8921517 and CHE-9300694) and U.S. Department of Energy (DE-FG02-90ER14143 and DE-FG02-90ER14143-A002). It is also a pleasure to acknowledge the skill and patience of those graduate students whose names appear in the citations from this laboratory.

1. J. R. Lakowicz, *Principles of Fluorescence Spectroscopy* (Plenum Press, New York, 1983).
2. *Topics in Fluorescence Spectroscopy*, J. R. Lakowicz, Ed. (Plenum Press, New York, 1991), Vol. 1–3.
3. J. N. Demas, *Excited State Lifetime Measurements* (Academic Press, New York, 1983).
4. I. M. Warner, G. Patonay, and M. P. Thomas, Anal. Chem. **57,** 463A (1985).
5. E. L. Wehry, Phys. Methods Chem. **8,** 109 (1993).
6. F. V. Bright, Anal. Chem. **60,** 1031A (1988).
7. S. A. Soper, L. B. McGown, and I. M. Warner, Anal. Chem. **66,** 428R (1994).
8. T. Vo-Dinh, Anal. Chem. **50,** 396 (1978).
9. L. Meites, *Handbook of Analytical Chemistry* (McGraw-Hill, New York, 1963), pp. 6–178.
10. D. C. Dong and M. A. Winnik, Can. J. Chem. **62,** 2560 (1984).
11. J. D. Andrade, V. Hlady, and A. P. Wei, Pure Appl. Chem. **64,** 1777 (1992).
12. D. C. Nguyen, R. A. Keller, J. H. Jett, and J. C. Martin, Anal. Chem. **59,** 2158 (1987).
13. M. D. Barnes, K. C. Ng, W. B. Whitten, and J. M. Ramsey, Anal. Chem. **65,** 2360 (1993).
14. C. D. Stubbs and A. D. Smith, Essays Biochem. **19,** 1 (1984).
15. V. M. Rangnekar, J. T. Foley, and P. B. Oldham, Appl. Spectrosc. **46,** 827 (1992).
16. L. Stryer and R. P. Haugland, Proc. Natl. Acad. Sci. **58,** 719 (1967).
17. M. C. Gutierrez, A. Gomez-Hens, and D. Perez-Bendito, Talanta **36,** 1187 (1989).
18. U. Narang, R. Wang, P. N. Prasad, and F. V. Bright, J. Phys. Chem. **98,** 17, 1994.
19. T. A. Betts, J. Zagrobelny, and F. V. Bright, J. Am. Chem. Soc. **114,** 8163 (1992).
20. D. V. O'Connor and D. Phillips, *Time-Correlated Single Photon Counting* (Academic Press, London, 1984).
21. D. R. James and W. R. Ware, Chem. Phys. Lett. **120,** 455 (1985).
22. J. R. Alcala, E. Gratton, and F. G. Prendergast, Biophys. J. **51,** 597 (1987).
23. D. J. S. Birch and R. E. Imhof, in *Topics in Fluorescence Spectroscopy*, J. R. Lakowicz, Ed. (Plenum Press, New York, 1991), Vol. 1, Chapter 1.
24. E. Gratton, D. M. Jameson, and R. D. Hall, Annu. Rev. Biophys. Bioeng. **13,** 105 (1984).
25. F. V. Bright, T. A. Betts, and K. S. Litwiler, C. R. C. Crit. Rev. Anal. Chem. **21,** 389 (1990).
26. J. R. Lakowicz and I. Gryczynski, in *Topics in Fluorescence Spectroscopy*, J. R. Lakowicz, Ed. (Plenum Press, New York, 1991), Vol. 1, Chap. 5.
27. A. P. Demchenko, *Ultraviolet Spectroscopy of Proteins* (Springer-Verlag, Berlin, 1986).
28. M. Maroncelli, J. MacInnis, and G. R. Fleming, Science **243,** 1674 (1989).
29. A. Muñoz de la Peña, T. T. Ndou, and I. M. Warner, in *Advances in Multidimensional Luminescence*, I. M. Warner and L. B. McGown, Eds. (JAI Press, Greenwich, State 1993), Vol. 2, p. 1.
30. K. Kondo and J. H. Fendler, Biochim. Biophys. Acta **509,** 289 (1978).
31. J. M. Beechem, M. Ameloot, and L. Brand, Chem. Phys. Lett. **120,** 466 (1985).
32. M. R. Eftink, in *Topics in Fluorescence Spectroscopy*, J. R. Lakowicz, Ed. (Plenum Press, New York, 1991), Vol. 2, Chap. 5642.
33. A. L. Wong and J. M. Harris, J. Phys. Chem. **95,** 5895 (1991).
34. M. A. Winnik, Acc. Chem. Res. **18,** 73 (1985).
35. F. V. Bright, Appl. Spectrosc. **47,** 1152 (1993).
36. F. V. Bright, R. Wang, M. Li, and R. A. Dunbar, Immunomethods **3,** 104 (1993).
37. J. S. Lundgren, E. J. Bekos, R. Wang, and F. V. Bright, Anal. Chem. **66,** 2433 (1994).
38. J. Zagrobelny, T. A. Betts, and F. V. Bright, J. Am. Chem. Soc. **114,** 5249 (1992).
39. J. K. Rice, S. J. Christopher, U. Narang, W. R. Peifer, and F. V. Bright, Analyst **119,** 505 (1994).
40. D. Ben-Amotz and J. M. Drake, J. Chem. Phys. **89,** 1019 (1988).
41. I. Gryczynski, H. Cherek, and J. R. Lakowicz, Biophys. Chem. **30,** 271 (1988).
42. J. Yguerbide, H. F. Epstein, and L. Stryer, J. Mol. Biol. **51,** 573 (1970).
43. R. Wang and F. V. Bright, J. Phys. Chem. **97,** 4231 (1993).
44. R. Wang and F. V. Bright, J. Phys. Chem. **97,** 10872 (1993).
45. M. J. Wirth and J. D. Burbage, Anal. Chem. **63,** 1311 (1991).
46. D. W. Pierce and S. G. Boxer, J. Phys. Chem. **96,** 5560 (1992).
47. R. Wang, S. Sun, E. J. Bekos, and F. V. Bright, Anal. Chem., paper in press.